J. Membrane Biol. 73, 263–274 (1983)

The Journal of
Membrane Biology

Bicarbonate Transport in *Chara corallina*: Evidence for Cotransport of HCO_3^- with H^+

William J. Lucas, David W. Keifer and Dale Sanders*
Department of Botany, University of California, Davis, California 95616

Summary. Experiments were undertaken on the fresh water alga *Chara corallina* to determine the form of inorganic carbon (CO_2 or HCO_3^-) which enters the cell during photosynthesis at alkaline pH. Recent proposals have centered on the possibility that proton efflux in alkaline solution is able to generate, in the immediate vicinity of the cell, a sufficiently low pH to raise the partial pressure of CO_2, and hence facilitate its passive permeation into the cell. Predictions have been made by modelling this situation (N.A. Walker, F.A. Smith & I.R. Cathers, 1980, *J. Membrane Biol.* **57**:51–58, J.M. Ferrier, 1980, *Plant Physiol.* **66**:1198–1199), and these were tested by placing recessed-tip pH microelectrodes in the unstirred layer surrounding cells in stagnant solution (bulk pH 8.2, buffered only with 1 mM HCO_3^-). Even as close as 2 μm from the cell wall, the pH was typically 7.2 to 7.6 in the acid band center – over 1 pH unit *greater* than that suggested by the models for CO_2 entry at the necessary rate for C-fixation. Further evidence for the entry of HCO_3^-, rather than CO_2, at high solution pH was obtained from experiments in which the radial pH gradient in the unstirred layer was reduced. Buffer solutions containing 5 mM phosphate or 5 mM HEPES, raised the pH at the cell surface in the acid regions from around 7.2 to 7.8 or higher. This pH increase (reduction in acid gradient) would have greatly reduced the CO_2 level at the cell surface and should, therefore, have greatly reduced the CO_2-related ^{14}C-influx. However, ^{14}C-fixation was reduced by only 31% (phosphate) or 15% (HEPES), compared with buffer-free controls. Reduction of the unstirred layer thickness by fast solution flow resulted in a stimulation, and not a reduction, of ^{14}C-fixation. The similarity of our radial pH profiles near the wall with that predicted by the model (Walker et al., 1980) assuming $H^+ - HCO_3^-$ cotransport, together with the effects of buffer, and the results of increased solution flow rate, lead to the conclusion that cotransport of HCO_3^- with H^+ is the likely method of entry of inorganic carbon. Longitudinal pH profiles of the *Chara* cell were obtained at a distance of 25 μm from the wall. These revealed much sharper delineation of the acid and alkaline bands than has previously been possible with miniature pH electrodes. Profiles of local electric field, obtained with a vibrating probe, were in excellent agreement with the high resolution pH profiles. This supports the hypothesis that membrane proton transport has a role (direct) in the generation of the extracellular currents.

Key Words *Chara* · bicarbonate transport · extracellular pH · recessed-tip pH microelectrodes

* *Current address:* Department of Physiology, Yale University School of Medicine, New Haven, Connecticut 06510.

Introduction

The topic of photosynthetic assimilation of exogenous HCO_3^- by aquatic plants has indeed been controversial. However, there are numerous reports in the literature which purport to demonstrate that certain algae and aquatic angiosperms can utilize the inorganic carbon of exogenous HCO_3^- for photosynthesis (Arens, 1933, 1936; Ruttner, 1947; Steemann-Nielsen, 1947, 1960; Österlind, 1949; Raven, 1968, 1970; Lucas, 1975). The main difficulty in the interpretation of the results pertaining to HCO_3^- assimilation is the fact that HCO_3^- may act as a reservoir for extracellular CO_2. Hood and Park (1962) attempted to remove the CO_2 from the HCO_3^- solution and hence determine whether photosynthetic fixation still proceeded. This approach was justifiably criticized by Watt and Paasche (1963) and Steemann-Nielsen (1963).

Raven (1968, 1970) developed a more rigorous form of analysis to ascertain whether a species could utilize exogenous HCO_3^-. The approach consisted of comparing fixation at high external pH (where membrane transport appears to be the rate-limiting step) with that at low pH, where most of the inorganic carbon is in the molecular form. If the cell is unable to transport bicarbonate, then at a given total carbon concentration fixation should vary with the external proton concentration, since this parameter will determine the concentration of CO_2 present. In fact, much higher levels of fixation were found at alkaline pH than could be accounted for by the presumed concentration of molecular CO_2, and this led Smith (1968), and later Lucas (1975) to propose that internodal cells of *Chara corallina* could transport HCO_3^-. Lucas (1975) also showed, on theoretical grounds, that the rate of CO_2 supply from the pool of HCO_3^- could not match the rates of ^{14}C-fixation

observed in alkaline media. Similar theoretical analyses have been reported for *Microcystis aeruginosa* and *Ceratium hirudinella* (Talling, 1976), *Egeria densa* (Browse, Dromgoole & Brown, 1979) and *Coccochloris peniocystis* (Miller & Colman, 1980).

However, the above approach does not take into consideration the possibility that an acidic unstirred layer might exist around the cell, even in alkaline media, due to the activity of the outwardly directed H^+ pump (Spanswick, 1981). This has prompted several groups to suggest that in this locally acidic region, the molecular CO_2 concentration may be significantly higher than that estimated from measurements in the bulk medium, and that in reality, aquatic angiosperms and Characean algae may not have the capability to transport HCO_3^- (Prins et al., 1979, 1980, 1982; Ferrier, 1980; Smith & Walker, 1980; Walker et al., 1980). Two independent attempts to quantify these ideas have led to the notion that the pH at the membrane (cell surface) should be about 6.0 or lower in order to attain the observed rates of ^{14}C-fixation in media of bulk pH 8.2 or above (Ferrier, 1980; Walker et al., 1980).

It is clear that a critical discrimination between these hypotheses must come from measurement of the pH in the unstirred layer, and as close as possible to the cell wall. Until recently, good spatial resolution of the radial pH profile has not been possible, because the miniature pH electrodes used for such studies had pH-sensitive areas about as large as the unstirred layer itself. However, with the advent of pH microelectrodes, it has now become possible to measure the pH inside the unstirred layer. From these observations, we have been able to conclude that in *Chara* HCO_3^- transport, and not permeation of molecular CO_2, appears to be the major mode of carbon uptake under alkaline conditions.

Besides the possibility that CO_2 is the predominant permeant species at all external pH values, Walker et al. (1980) also considered, quantitatively, the effects of two alternative modes of HCO_3^- transport on the pH of the unstirred layer. For both HCO_3^- uniport and for $HCO_3^- - H^+$ cotransport, some acidification near the cell wall is expected, although low pH in the unstirred layer is a consequence of, and not a requirement for, transport in either case. On the other hand, changing the pH of the unstirred layer should have a different effect on the HCO_3^- flux depending on the mode of entry. For a uniport mechanism, raising the pH of the unstirred layer from 7.2 to 7.8 should slightly *increase* the HCO_3^- flux, whereas a more complex effect is expected for $HCO_3^- - H^+$ cotransport. In the present work, we have tried to discriminate between these two possibilities by adjusting the pH in the unstirred layer either with buffers, or with fast flowing solutions.

Materials and Methods

Plant Material

Culture material of *Chara corallina* Klein ex Willd., em. R.D.W. (= *C. australis* R. Br.) was grown in the laboratory in two large containers (A: 80 liters, B: 45 liters). The solution in A initially contained (mM): 3.0 Na^+, 0.2 K^+, 0.2 Ca^{2+}, 0.2 SO_4^{2-}, 1.2 Cl^- and 2.0 HCO_3^-, pH 8.5 to 9.5; the solution in B contained: 6.0 Na^+, 0.2 K^+, 0.2 Ca^{2+}, 0.2 SO_4^{2-}, 1.2 Cl^-, 2.0 HCO_3^- and 2 mM N-2-hydroxyethyl-piperazine-N′-2-ethanesulfonic acid (HEPES) at pH 7.5. Both systems were illuminated (14 h light) with fluorescent lighting (Sylvania, Lifeline, F30T12-CW-RS or F48-CW-RS) with the intensity at the solution surface being 17 to 20 W m^{-2}. All experiments were performed on mature male internodal cells that were cut from the main axis of the vegetative shoot one or two days prior to being used in an experiment.

Recessed-Tip pH and Extracellular Current Measurements

Excised internodal cells were rinsed in an artificial pond medium [CPW/B, containing (mM): 1.0 NaCl, 0.2 KCl, 0.2 $CaSO_4$, 1.0 $NaHCO_3$ (pH 8.0 to 8.2)] and then cellular debris was removed from the cut ends of the branch- and adjoining internodal-cells using a Pasteur pipette to which a partial vacuum had been applied. During initial experiments with the miniature pH electrode we used the agar-block technique (Lucas & Smith, 1973) to measure the steady-state pH profile along the *Chara* cell wall. [The agar blocks were used as embedding media for experimental cells, and were prepared in a manner similar to that described by Lucas and Dainty (1977).] Cells were pretreated in CPW/B (20 W m^{-2}) for 1 to 2 h to establish a stable pH profile near the cell wall. It should be mentioned that we conducted all surface pH experiments in the presence of 1 mM total inorganic carbon to allow a direct comparison between our results and the theoretical data obtained by Walker et al. (1980) and Ferrier (1980). For the agar-block system, the pH measurements were made using a miniature pH electrode (Microelectrodes, Inc., Londondery, New Hampshire, Model MI-405) in conjunction with a Beckman 4500 digital pH meter. A Leitz micromanipulator was used to position, and traverse, the pH electrode along the *Chara* cell wall. From the values obtained the pH pattern established near the cell surface was mapped.

The *Chara* internodal cell was then removed from the agar block and silk threads (Type: Orizuru 9; Kanagawa Co. Ltd., Kanagawa, Japan) were attached to the dead cell wall-fragments of the adjoining internodal cells. These silk threads were then used to suspend the cell in the center of a 9-mm-deep, 30-mm-wide and 56-mm-long Plexiglas chamber filled with CPW/B. Small Plexiglas blocks (height 4.5 mm) were placed beneath the threads near the ends of the cell to stabilize the cell's position. (A mature antheridium was used to orient the internodal cell such that the same cell wall regions could be scanned with both the miniature and micro pH electrodes.) Cells mounted in this manner were stored, overnight, in a covered petri dish.

On the following day, the Plexiglas chamber containing the suspended *Chara* cell was placed on the stage of a compound inverted microscope (Invertoscope D; Zeiss, New York) and the cell illuminated (20 W m^{-2}) using a bifurcated fiber optic light source (model MK II; Ehrenreigh Photo Optical Industries, Inc., Garden City, New York). The microscope stage was motorized (stepping motor, model KD 3402-004; Hurst Manufacturing Corp., Princeton, Indiana, coupled to a model SL 10 adjustable speed controller; Minarik Electric Co., Los Angeles, Calif.) so that the entire length of the *Chara* cell could be traversed past either the vibrating electrode or recessed-tip pH microelectrode.

After a 2-h illumination period the extracellular currents near the cell wall were measured using the vibrating probe system developed by Jaffe and Nuccitelli (1974). Full details of the application of this technique to the *Chara* system have been reported by Lucas and Nuccitelli (1980). In the present study we adopted the same basic procedures, with the following exceptions. All measurements were made using a spherical platinum-black electrode with a tip diameter of approximately 10 μm. The electrode was vibrated over a distance of 12.5 μm at a frequency of 328 Hz; the vibrating electrode was maintained at a distance of 50 ± 5 μm from the cell surface.

Using the measured conductivity of the solution, the potentials obtained from the vibrating probe were converted to local current densities (μA cm^{-2}), and these were converted to flux densities by dividing by Faraday's constant (*see* Lucas & Nuccitelli, 1980). All vibrating probe data are presented in terms of flux densities, in units of pmol cm^{-2} s^{-1}. The convention followed was to display inward current, which occurred in the alkaline regions, as positive fluxes, and the outward current which occurred in the acid regions as negative fluxes.

After current scans were completed, the vibrating probe assembly was removed and replaced by the recessed-tip pH microelectrode system; *Chara* cells were allowed approximately 1 h to re-equilibrate before making pH measurements. The motorized stage was used to position the *Chara* cell, and a micromanipulator (Model H-2; Line-Tool, Allentown, Pa.) was used to adjust the position of the pH microelectrode. Recessed-tip electrodes were fabricated according to the method of Thomas (1978) with their dimensions optimized for rapid response (*see* Sanders & Slayman, 1982). Generally, the time constants of the electrodes in response to a step change in pH in buffered solutions were on the order of 5 to 20 s, with a sensitivity of greater than 55 mV/pH unit. The length of exposed pH glass in most cases was 35 μm, and the tip diameter was 0.5 μm. The reference electrode was a broken-tipped microelectrode (tip diameter, about 10 μm), filled with 1 M KCl in 2% agar. In order to prevent perturbation by leaking KCl under these stagnant conditions the reference electrode was positioned at least 2 cm from the cell. The output from the pH electrode was fed into a high impedence (10^{14} ohm) amplifier (constructed by Bob Sind, Washington University Medical School, St. Louis, Missouri) and readings were made from a digital meter. Since, in these experiments, we were only interested in steady-state pH gradients, a single pH value was recorded for each position of the electrode after the reading had stabilized, as determined from recordings on a Hewlett-Packard (Model 7132A) chart recorder. Usually, stabilization required a few minutes, probably due to slight solution mixing during the movement of the electrode. Periodically during an experiment, the electrode was repositioned to a site for which the pH had already been determined, in order to check for time-dependent drift. However, in spite of the rather lengthy duration of the experiments (about 3 to 4 h), the measured values and patterns were quite stable. All manipulations were observed under 200 × magnification. Longitudinal scans of extracellular pH were performed with the electrode tip 25 μm from the cell surface. In some experiments, radial scans were then made at specific locations along the cell, pH values being obtained as close as 2 μm from the cell wall. During all pH microelectrode measurements the upper solution surface was partially covered, with the aid of several large glass coverslips, to reduce convection currents and CO_2 loss from the solution.

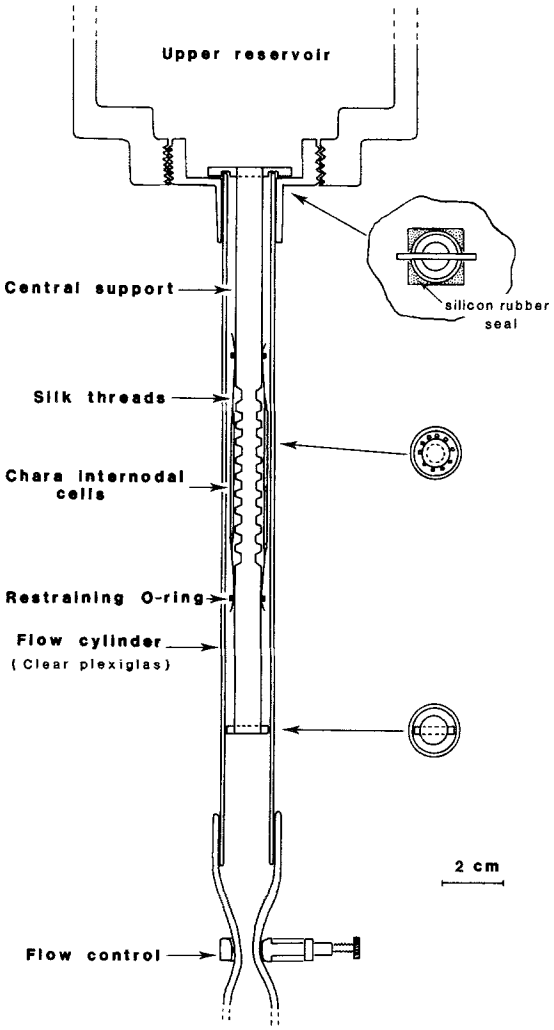

Fig. 1. Schematic representation of the apparatus used to vary the width of the *Chara* cell unstirred layer. The *Chara* internodal cells were attached to a clear Plexiglas central support via silk threads and restraining O-rings. This support fitted into a flow cylinder which screwed into an upper reservoir and was connected, via Tygon tubing, to a lower reservoir (4.5 liter total volume). Experimental solution was pumped from the lower to the upper reservoir and the flow rate past the cells was adjusted using a screw clamp; excess volume within the upper cylinder was returned via a bypass. The position of the bypass valve was such that a constant hydrostatic head of 80 cms was maintained for all experiments

Flowing Solution Experiments

The apparatus illustrated in Fig. 1 was used to investigate the effect of the unstirred layer thickness on the rate of $H^{14}CO_3^-$ assimilation. For these experiments, cells were cut from the

culture and their lengths and diameter measured to enable surface area computation. Silk threads were then attached to the cells (*see above*) and these threads were used to anchor the cells onto the central support (*see* Fig. 1). The mounted cells were given an overnight pretreatment in CPW/B (0.5 HCO_3^-) before being used in flow experiments. The general procedure used in these experiments was as follows. The central support, with the mounted cells, was transferred to the flow cylinder, which contained solution, and this unit was quickly screwed into the upper reservoir housing (*see* Fig. 1). The lower reservoir originally contained 3 liters of CPW/0.5 $NaHCO_3$ and this was circulated through the system by means of a Teflon-sealed impeller-driven pump (model 1P681 Teel; Dayton Electric Manufacturing Co., Chicago, Ill.). All cells were pretreated for 1 h under 20 W m^{-2}, 25 °C at the flow rate used during the ^{14}C uptake experiment. The period of $H^{14}CO_3^-$ exposure (30 min) was initiated by injecting 50 µl of stock $NaH^{14}CO_3$ solution (47 mCi/mmol; New England Nuclear) into the lower reservoir. Preliminary experiments indicated that the upper and lower reservoirs become uniformly labeled in less than 30 s at high flow rates; at lower flow rates stirring within the two reservoirs accomplished this uniform mixing.

The specific activity of the solution did not change significantly throughout the course of an experiment, as determined from aliquots of the ^{14}C-solution obtained about 2 min after adding isotope and just before uptake was terminated. The solution pH, 8.4 at the start of the experiment, decreased by 0.4 units, or less, over the 90-min experimental period.

At the end of an isotope treatment the cells were removed from the flow cylinder, the silk threads severed, and the cells rinsed before being bathed for 5 min in CPW/B to remove external ^{14}C. Individual cells were then blotted and placed in scintillation vials where they were treated (60 min) with 0.1 ml of 30% H_2O_2 and 0.1 ml of 7% perchloric acid to digest the tissue, prevent chlorophyll quenching during scintillation counting and remove unfixed ^{14}C. Tissue was suspended in 10 ml of Beckman Filtersolv and radioactivity measured in a Beckman LS 9800 liquid scintillation system. Influx into each cell was calculated using its measured surface area. Each treatment consisted of 10 cells. Results are reported as: average ±SE.

Results

Miniature Versus Micro pH Electrode Measurements

Our initial experiments were directed towards comparing the *Chara* cell wall pH profiles that were measured with a miniature pH electrode and a recessed-tip pH microelectrode. Figure 2 illustrates the striking difference observed between the pH profiles measured by the two pH electrodes; in the alkaline regions the profiles were quite similar, but in the HCO_3^--transporting regions, only the recessed-tip pH microelectrode detected acidification of the medium to values below the pH of the bulk solution. Clearly, Walker et al. (1980) were corrected in their assessment that the miniature electrode was too large to accurately measure the localized pH gradients that develop within the immediate vicinity of the cell surface.

Experiments were also conducted in which we utilized the vibrating probe technique in conjunction with the miniature and micro pH electrodes

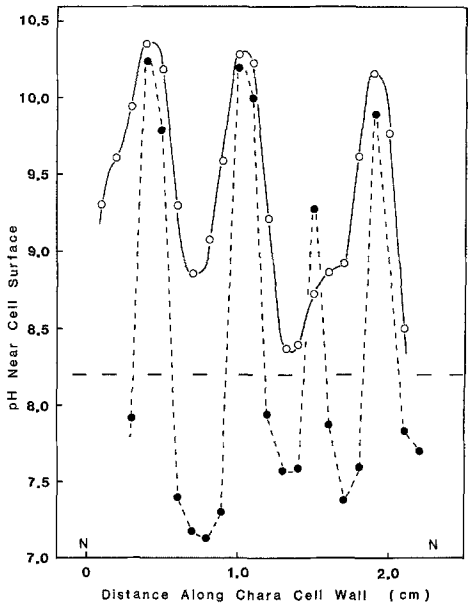

Fig. 2. Comparative pH profiles measured near the surface of *Chara* internodal cells during photosynthetic assimilation of exogenous HCO_3^-. Measurements were made using a miniature pH electrode (o) and a recessed-tip pH microelectrode (•). The miniature pH electrode was positioned such that the tip of the hemispherical electrode just touched the cell surface, while the tip of the pH microelectrode was maintained at a distance of 25 µm from the cell wall. The horizontal broken line represents the pH value of the bathing medium and the symbol *N* indicates the position of the nodes

(Fig. 3). From these studies we found an excellent correlation, within any given cell, between the profiles of current density and of pH, measured with the microelectrode (*cf.* Fig. 3*A* & *B*). For the cell in Fig. 3, for example, the current density in the acid bands indicates electrogenic fluxes of 120 to 170 pmol cm^{-2} s^{-1}. If this current were entirely due to H^+ efflux, then this would be slightly larger than the H^+ efflux of 100 pmol cm^{-2} s^{-1} used in the models for formation of sufficient extracellular CO_2 (Ferrier, 1980; Walker et al., 1980) for uptake solely as CO_2. However, even if H^+ efflux is solely responsible for this electrogenic activity, it is clear that the pH value 25 µm from the cell wall (7.2 to 7.6) is substantially higher than the theoretical value (about 6.0) obtained from the models of Walker et al. (1980) and Ferrier (1980). Indeed, as the radial pH profile in Fig. 3*C* shows, we were unable to measure a pH value of less than 7.2 with the pH microelectrode positioned only 2 µm from the cell wall. In only one experiment of all those conducted did we measure a lower pH value. A major conclusion is, therefore, that the proton concentration at the cell wall appears to be at least 10-fold too low to yield sufficient CO_2 for the observed rates of photosynthesis at this pH value.

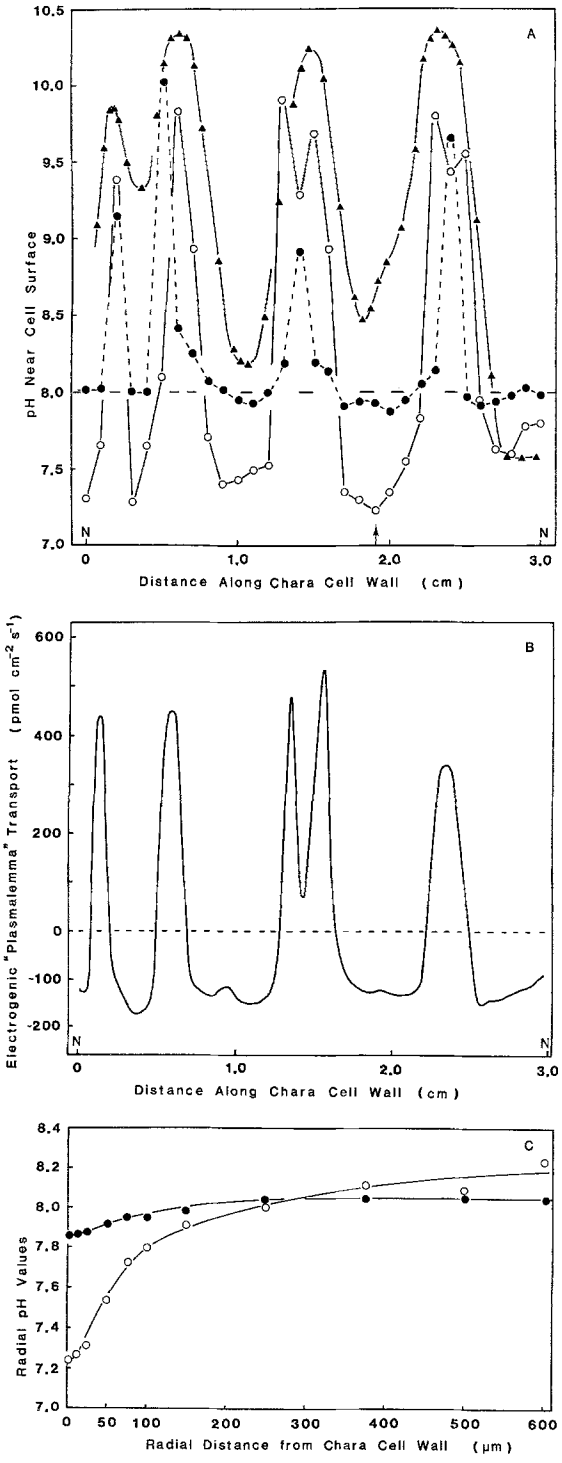

Fig. 3. Correlation between cell surface and radial pH profiles obtained along a *Chara* cell and the extracellular currents that were measured using the vibrating probe technique. *A:* Cell surface pH profiles measured using either a miniature pH electrode (▲) or a recessed-tip pH microelectrode (○). Micro pH electrode measurements were also made in CPW/B medium containing 5 mM phosphate buffer (●). Arrow indicates the position at which radial pH profiles were obtained (*see C*). *B:* Extracellular vibrating probe scan conducted on the same cell. *C:* Radial pH scans obtained using a recessed-tip pH microelectrode; ○, medium contained CPW/B; ●, CPW/B medium buffered by 5 mM phosphate

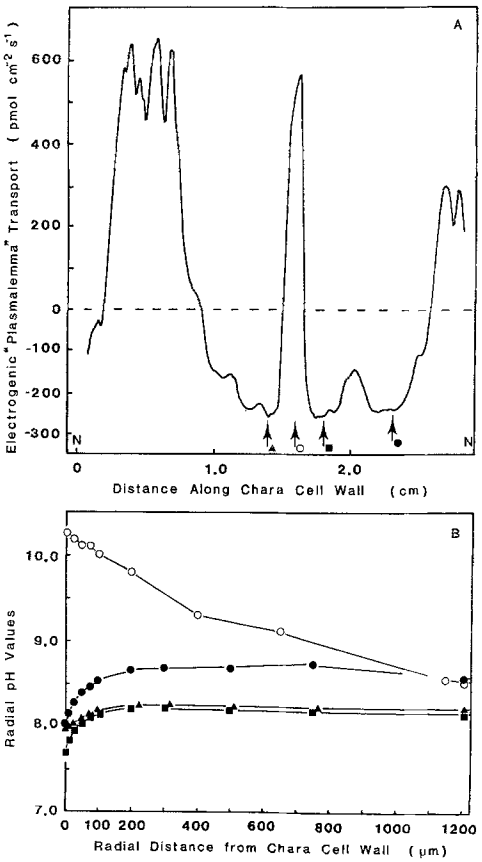

Fig. 4. Extracellular current (*A*) and radial pH profiles (*B*) measured on a *Chara* internodal cell bathed in CPW/B. The spatial positions along the cell at which the radial profiles were obtained are indicated by arrows in *A*

If the CO_2 permeation hypothesis were correct, then the observed currents in the acid bands (which would be due to H^+ efflux across the plasmalemma) should be positively correlated with the pH value at the cell surface. Comparison of the radial pH profiles and current scans for the two cells in Figs. 3 and 4 shows that this is not the case. In Fig. 3*C*, the pH value of the cell surface was 7.22, in a region where the outward current indicates the presence of an electrogenic flux of 130 pmol cm^{-2} s^{-1}, whereas in Fig. 4*B*, the pH was never below 7.65 and yet the electrogenic flux was 250 pmol cm^{-2} s^{-1}. However, the interpretation of these pH values is complicated by the increase in pH that would be caused by CO_2 leaving the HCO_3^- solution and entering the cell. The ionic identity of this outward current is considered in the Discussion.

Influence of Artificial Buffers on the pH and Extracellular Current Profiles

Inclusion of 5 mM HPO_4^{2-} (pK = 7.2) or HEPES (pK = 7.55) buffer in the CPW/B significantly

Table 1. Effect of exogenous buffers on ^{14}C-fixation in *Chara corallina*[a]

Treatment	^{14}C Fixation (pmol cm^{-2} s^{-1})	% of Control
Control, unbuffered (except for 1.0 mM $NaHCO_3$)	39±2	–
5 mM Phosphate buffer	27±1	69
10 mM Phosphate buffer	27±2	69
5 mM HEPES	33±2	85
10 mM HEPES	28±1	71

[a] Photosynthetic fixation was measured from ^{14}C incorporated during a 10-min uptake period in CPW/B, pH 8.2 (25 C and 20 W m^{-2}). In addition, the solution contained the buffer indicated in the Table. Values represent the mean ±SE; twelve cells were used per treatment

reduced the cell surface pH profiles, with the acid regions being influenced more so than the alkaline regions (Fig. 3*A*). As expected, this level of buffer significantly dissipated the radial pH gradients (Fig. 3*C*). According to the CO_2-production model, raising the pH value at the cell surface would reduce the concentration (and hence the flux) of CO_2 (Walker et al., 1980, Fig. 6). Therefore, the buffer should dramatically reduce the rate of ^{14}C fixation. The results presented in Table 1 indicate that photosynthesis was reduced when *Chara* cells were bathed in artificial buffer. However, levels of buffer which caused the proton concentration at the cell surface to be reduced by a factor greater than 4 (pH change from 7.22 to 7.84 in Fig. 3*C*) resulted in only a 30% reduction in ^{14}C fixation. The origins of this reduction are considered in the Discussion.

The influence of buffering the bathing medium on the extracellular currents was next examined. Since photosynthesis was reduced when cells were exposed to buffered medium, we anticipated that the extracellular currents would reflect this inhibition. A comparison of vibrating probe scans obtained under control (CPW/B) and buffered (CPW/B, plus 5 mM HPO_4^{2-}) conditions revealed that this was not the case (Fig. 5). The extracellular currents in the acid regions were unaffected by the presence or absence of buffer (either HPO_4^{2-} or HEPES at 5 to 10 mM). The total OH^- current of the cell was also unaffected, but at times there seemed to be a slight redistribution of the OH^- fluxes between the various alkaline bands.

Reduction of the Unstirred Layer

Walker et al. (1980) suggested that extracellular production of CO_2 would be highly efficient in the environment of the *Chara* cell, "because the

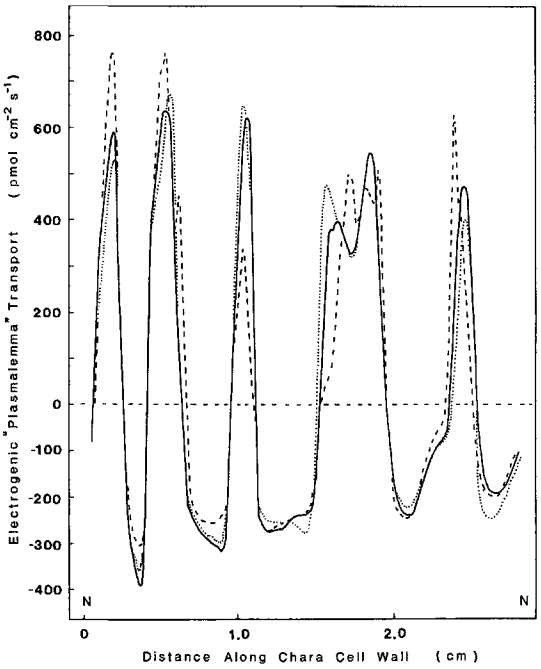

Fig. 5. Influence of artificial buffer on the extracellular currents that develop along the *Chara* cell during HCO_3^- assimilation. The solid and dotted traces are representative control scans obtained when the cell was bathed in CPW/B. The broken trace is a typical scan obtained when the medium was buffered by 5 mM Na_2HPO_4

diffusion resistance of the unstirred layer retains the CO_2 that is produced near the cell surface, and the H^+ that flow out from the cell." Hence, an explicit prediction of the CO_2-production model would be that a reduction in the unstirred layer could cause a decline in the rate of photosynthesis. To test this prediction, we built a system that allowed us to vary the rate at which the experimental solution flowed past the *Chara* cell surface (*see* Fig. 1). Since we knew that HCO_3^- assimilation in *C. corallina* is easily perturbed (*see*, e.g., Lucas & Nuccitelli, 1980), we took considerable care in the development of the protocol used in these experiments (*see* Materials and Methods). The results of these experiments are presented in Fig. 6. Under stagnant solution conditions we found the same rate of $H^{14}CO_3^-$ assimilation as obtained when we used our previous system (Lucas, 1975; Lucas & Dainty, 1977). The influence of solution flow, as a pretreatment, was investigated in a control experiment by exposing cells to a flow rate of 1.76 liters per min for 1 h and then measuring ^{14}C assimilation under stagnant conditions (Fig. 6, △). There did appear to be a slight perturbative effect on assimilation, but it was not serious. As the flow of experimental solution was increased, the rate of ^{14}C assimilation underwent an increase, not a

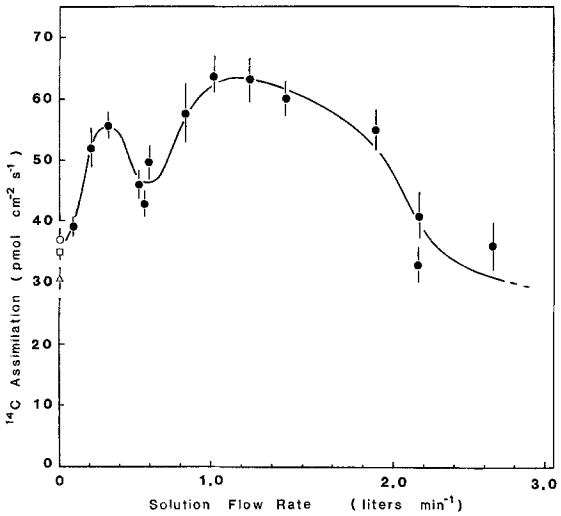

Fig. 6. Effect of reducing the unstirred layer on ^{14}C assimilation in *Chara* internodal cells. The apparatus illustrated in Fig. 1 was used to conduct experiment under both stagnant (o) and flowing (•) solution conditions. All measurements were performed in the presence of 0.5 mM total inorganic carbon. The symbol, □, represents ^{14}C assimilation measured using the technique of Lucas (1975). In one experiment (△), cells were pretreated for 1 h in flowing solution (1.76 liters per min) and then ^{14}C assimilation was measured in a stagnant solution. In all other experiments, pretreatment (1 h) and $H^{14}CO_3^-$ exposure (30 min) were at the indicated rate of solution flow. (Values represent the mean and SE for 10 cells.)

decrease. Intermediate flow rates resulted in a transient decrease in ^{14}C fixation, back towards the stagnant-solution values, with a subsequent recovery at the higher flow rates; at very high flow rates ^{14}C fixation again declined.

Flow Velocity Near the Cell Wall

In correlating the ^{14}C-fixation rate with the rate of volume flow through the experimental system (Fig. 6), it is important to know the actual flow velocities near the cell surface. By making the assumption that the cells mounted in the fast flow chamber do not significantly alter the chamber geometry, our system can be approximated as fluid flow through the annulus between two concentric round tubes. This geometry has been treated in many texts on fluid dynamics (*see*, e.g., Streeter, 1958) and from the equations so derived the velocity (U) of fluid flow, at a distance x from the inner surface, can be given in terms of the fluid volume flow rate Q:

$$\frac{U(x)}{Q}=\frac{2}{\pi}\frac{a^2-b^2-2bx-x^2+\dfrac{a^2-b^2}{\ln b/a}\ln\dfrac{a}{(b+x)}}{(a^2-b^2)(a^2+b^2)-(a^2-b^2)^2/\ln a/b} \quad (1)$$

where a and b are the radii of the inner and outer surfaces, respectively. In our system $a=0.47$ cm and $b=0.79$ cm, thus for $U(x)$ in cm/s, Q needs to be in ml/s. For small values of x (<0.01 cm), this relationship can be reduced to: $U(x)/Q=16.4x$. This says, for example, that if the flow rate through the chamber is 1 liter/min (16.7 ml/s) the fluid flow 50 μm from the cell surface is 1.34 cm/s. These calculations apply, of course, only to the surface of the cell facing the fluid flow; the flow rate on the side facing the central support would be greatly reduced. Relating this flow velocity to an unstirred layer thickness is difficult, because the unstirred layer thickness is not defined in terms of the flow rate. But if we assume that the unstirred layer thickness would be the distance from the cell where the permeability rate (P) by diffusion through that layer is comparable to the flow velocity component perpendicular to the cell at that point, then we can define such a thickness. Further, if the fluid flow has a component of flow perpendicular to the cell that is 1% of the flow parallel to the surface, $U(x)$, (probably an underestimate), then: $P=D/x=0.01\ U(x)=(0.01)\ (16.4)Qx$, where $D=$ diffusion coefficient $=1.1\times10^{-5}$ cm/s for HCO_3^- in aqueous solution (Walker et al., 1980), with the other terms as defined above. This can be rearranged to give:

$$x=\left(\frac{D}{0.16\,Q}\right)^{\frac{1}{2}}. \quad (2)$$

We see that the unstirred layer thickness is inversely proportional to the square root of the flow rate. For the above example (1 liter/min flow rate), this gives an unstirred layer thickness of approximately 20 μm. If the perpendicular component of flow were larger, say 4% of the parallel flow, then the unstirred layer thickness would be reduced to 10 μm in this example.

Discussion

Evidence Against the CO_2 Model

The present results clearly indicate that in alkaline media (pH 8 to 9) *Chara* internodal cells acidify regions along the cell wall, and these regions are coincident with the areas along the wall where we detected HCO_3^--associated currents (Fig. 3*A* & *B*). At first sight these findings appear to offer experimental support for the theoretical CO_2-generating model forwarded by Ferrier (1980) and Walker et al. (1980). However, a detailed comparison between our experimental findings and the predictions of the theoretical model(s) indicate that the

model is invalid. First, the CO_2 model suggests that the pH value at the *Chara* cell should be 6.0 in order for CO_2 to be produced at rates consistent with experimentally determined rates of photosynthesis (i.e. rates under alkaline conditions). We were unable to detect this level of acidification. Indeed, the pH value 2 μm from the cell wall was seldom lower than 7.2 (*compare* Fig. 3*C* with Fig. 3 of Walker et al., 1980). Second, the CO_2 model proposes that the outward current in the acid regions is due to electrogenic H^+ efflux. If this were the case, we would expect to find a relationship between the electrogenic fluxes (currents) in the acid regions and the level of surface acidification (only slightly complicated by the proposed entry of CO_2 into the cell), when comparing different cells. However, as shown in Figs. 3 and 4, we could find no such correlation. Although the HCO_3^--associated currents were stable, the degree of cell surface acidification was quite variable. Third, raising the pH value within the unstirred layer, by means of a buffer did not result in a dramatic reduction in ^{14}C-fixation (Table). The CO_2 model predicts that production of exogenous CO_2, and hence ^{14}C-fixation, would be sensitive to alteration of cell surface pH by exogenous buffer. The reason for the partial inhibition of photosynthesis, observed in the presence of buffer, will be discussed in a later section. Finally, if CO_2 molecules were actually being produced in the unstirred layer, then flowing solution past the cell surface should deplete the CO_2 available for diffusion into the cell; i.e. photosynthesis should be reduced under flowing-solution conditions. Photosynthesis was actually enhanced under these conditions (Fig. 6), a result quite incompatible with the exogenous CO_2 production model.

Mitigating Circumstances for the CO_2 Model

There are several possibilities as to the reason(s) for the discrepancies between our experimental findings and the predictions of the CO_2 model. Basic differences exist between our experimental system and the numerical model used by Walker et al. (1980). In the theoretical model the boundary layer thickness was set at 1.0 mm, while in our system analysis of the radial pH profile suggests that the boundary layer was approximately 200 μm in width. The narrower unstirred layer should cause the radial pH profile to be both steeper and reduced in magnitude. Whereas our experimental gradients were reduced in magnitude, the gradients were not steeper. Walker et al. (1980) obtained a theoretical gradient of 1.3 pH units over the initial 100 μm distance out from the cell surface, and this value was for a H^+ pump rate of 100 pmol cm^{-2} s^{-1}. In our experiments, the measured pH gradients over this same distance were much less; e.g. in Fig. 3*C* the value was 0.55, and in Fig. 4*B* the values were approximately 0.25. The extracellular currents, in the region where these radial pH profiles were measured, were 130 (Fig. 3*C*) and 250 (Fig. 4*B*) pmol cm^{-2} s^{-1}; these values reinforce our point concerning the lack of correlation between the observed currents and pH gradients.

Walker et al. (1980) reported that if in their model "the conditions are modified to include a representation of the cell wall, the results are very similar." Thus, almost all of their computations ignored the influence of the wall. In the absence of evidence of the contrary, it would seem unwise for us to assume that the cell wall of this species is homogenous throughout its width and length. Actually, the level of heterogeneity of the plasmalemma with respect to both the frequency and complexity of the charasomes (Franceschi & Lucas, 1980) suggests that changes in cell wall properties, in response to localize membrane transport function, may indeed be possible. This view is supported by the recent report that the cell wall of *Anabaena variabilis* undergoes sub-structural modification when cells are grown under low CO_2 culture conditions (Marcus et al., 1982).

Mechanism of HCO_3^- Transport

Under alkaline conditions, exogenous carbon does not appear to cross the plasmalemma of *Chara* solely via a CO_2 diffusion mechanism. The issue to be dealt with now concerns the discrimination between electrogenic HCO_3^- uniport and the possibility of cotransport with H^+. The similarity between our measured surface pH and radial pH profiles (Figs. 3*C* and 4*B*) and those computed by Walker et al. (1980), assuming $HCO_3^- - H^+$ cotransport, offer support for the latter hypothesis. The partial inhibition of photosynthesis, observed when 5 or 10 mM buffer (HPO_4^{2-} or HEPES) was included in the medium (Table 1), is also consistent with a $HCO_3^- - H^+$ cotransport mechanism. Given that the pH value within the cell wall is near the pK of the buffers used, the conjugate base of the buffer could inhibit $H^{14}CO_3^-$ transport by competing for H^+. Walker et al. (1980) offered a similar explanation to account for the inhibition of photosynthesis that Lucas (1975) found at pH values above 9.5, and in the presence of such buffers as

Tris, tricine and TES (Lucas, 1977). A HCO_3^- uniport system should be stimulated by exogenous buffer, as the buffer would reduce the draw-down of the surface pH as HCO_3^- is taken up, and the buffer would facilitate diffusion of HCO_3^- through the unstirred layer. Hence, the observed inhibition appears to indicate that primary electrogenic HCO_3^- transport does not occur in *Chara* (Lucas, 1976; Walker & Smith, 1977; Ferrier & Lucas, 1979).

Interpreting the Flowing Solution Experiments

A $HCO_3^- - H^+$ cotransport system or a HCO_3^- electrogenic uniport system would respond to flowing solutions in at least three ways. First, a reduction in the unstirred layer would increase net photosynthesis by reducing the diffusion-limitation on the movement of substrate from the bathing medium to the plasmalemma. Second, flowing solutions would sweep away the OH^- ions that were being released across the plasmalemma within the alkaline bands. This would serve to contain the alkaline band-associated pH increase along the cell wall and, thereby, allow a larger membrane surface area to engage in HCO_3^- acquisition. Third, flowing solutions would keep the surface pH closer to that of the bulk pH. If cell surface acidification represents protons that have escaped being captured by the cotransport process(es), then flowing solution, by sweeping away protons, should reduce the efficiency of the $HCO_3^- - H^+$ cotransport process. It may be that relatively few protons are lost to the bulk solution, possibly due to confinement in the cell wall or within membrane structures like the charasomes (Franceschi & Lucas, 1980), where these protons are quickly transferred from the H^+-electrogenic pump to the $HCO_3^- - H^+$ cotransport system. Or alternatively, the H^+-translocating ATPase may not be the rate-limiting step in ^{14}C-acquisition. On the other hand, if the cell surface acidification represents a draw-down of solution pH as HCO_3^- is transported into the cell by a uniport mechanism, then flowing solution would stimulate uptake by reducing this pH draw-down. It is likely that the first two of these ways are more important than the third, so that the results of the flowing solution experiments, while clearly supporting HCO_3^- uptake, are at least consistent with the proposed $HCO_3^- - H^+$ cotransport process.

The shape of the ^{14}C-photosynthesis versus solution flow rate is intriguing. We have no simple explanation as to why the stimulation in photosynthesis decreased in the region of 0.5 liters per min, only to recover at higher flow rates. Although the cells were securely anchored to the central support, the flowing solutions could still induce individual cells to vibrate. Lucas and Nuccitelli (1980) found that *Chara* cells could be perturbed by certain frequency-amplitude combinations of the vibrating probe. The perturbing influence of the vibrating probe manifested itself in a dramatic change in the OH^- efflux pattern along the *Chara* cell surface. If, at a certain flow rate, the *Chara* cells responded in a similar manner to that observed by Lucas and Nuccitelli (1980), the reduction in photosynthesis may reflect a limit on photosynthesis imposed by a reduction or alteration of OH^- efflux.

Nature of the Extracellular Current(s) in the Acid Bands

Lucas and Nuccitelli (1980) showed that the extracellular current, in the acid regions of the *Chara* cell wall, was dependent upon the presence of exogenous HCO_3^-. If an electrogenic HCO_3^- uniport system were operating across the plasmalemma, the outward extracellular current in the steady state would be carried almost entirely by this anion. However, our present data is more consistent with the operation of a $HCO_3^- - H^+$ cotransport process, and, thus, the nature of the ionic fluxes responsible for the extracellular current in the acid region becomes a little more complex.

In the presence of 5 or 10 mM HPO_4^{2-} (or HEPES) buffer the extracellular current patterns were not reduced (Fig. 5), although photosynthesis, *per se*, was inhibited by approximately 30% (Table 1). Our interpretation is that competition for H^+ between the $HCO_3^- - H^+$ cotransport system and the exogenous buffer reduced HCO_3^- transport into the cells, so that photosynthesis was depressed. But H^+ efflux was not affected as the protons were carried away from the H^+-electrogenic pump by diffusion of the buffer. The buffer facilitates the movement of H^+ away from the cell surface by diffusing away from the membrane, through the unstirred layer, in the protonated form (Gutknecht & Tosteson, 1973). The result is a net flow of positive charge away from the cell. If the limitation on photosynthesis is the rate of the H^+-electrogenic pump, then the buffer, by carrying H^+ away from the cell, would reduce HCO_3^- uptake. But in the unstirred layer no change would be observed in the current, as the vibrating probe can not distinguish between a current of HCO_3^- and

a current of protonated buffer. This process depends on the rate of diffusion of the buffer; if a less mobile buffer were used, then it should be less effective at inhibiting ^{14}C-fixation. That is borne out by our data: at a concentration of 5 mM, HEPES (mol wt = 238) is less effective than is phosphate (mol wt = 96). With phosphate the inhibitory effect is already saturated by a 5 mM concentration; with HEPES it takes 10 mM to reach equivalent levels of inhibition.

In a recent study, Lucas (1982) found that the extracellular current in the HCO_3^--transporting region of the cell can be maintained in the absence of exogenous HCO_3^-, provided the HCO_3^- is replaced with 1 mM HPO_4^{2-}. Lucas (1982) concluded from this that the H^+translocating ATPase must be separate from the $HCO_3^- - H^+$ cotransport system and that it is possible to effectively decouple the two systems.

The Problems of Modelling this System

Throughout this paper we have constantly compared our experimental results with the mathematical modelling done by Ferrier (1980) and by Walker et al. (1980). Walker et al. (1980) specifically modelled the proposed $HCO_3^- - H^+$ cotransport system. In comparing our experimental data with their predicted radial pH profiles, we noted the similarities but the fit was less than perfect. There are at least two simplifying assumptions in their model(s) that could be the cause of these differences. First is the elimination of the cell wall from most of their modelling. Not only does the cell wall provide a reaction space where H^+ would be restricted from free exchange with the bulk solution, but there are the charasome structures (Francheschi & Lucas, 1980) that may be important. These charasomes are found at higher density in the acid bands (Franceschi & Lucas, 1980), the region where HCO_3^- (Lucas, 1976) and Cl^- (Spear, Barr & Barr, 1969) are taken up into Characean cells. Since *Nitella flexilis* exhibited the same acid and alkaline banding pattern but did not possess the charasome structure, Franceschi and Lucas (1980) suggested that the charasome may not be involved in HCO_3^- transport. It will be of considerable interest to conduct recessed-tip micro pH electrode studies on *Nitella* species to further test this hypothesis.

In the present study, we provide evidence that HCO_3^- is taken up by a H^+-cotransport system, as has been shown for Cl^- (Sanders, 1980). It could be that the charasome is a structure which makes these cotransport systems much more efficient (*see* Franceschi & Lucas, 1982). If this is so, then the analysis in Walker et al. (1980) of the relative efficiency of the transport models versus unstirred layer (Fig. 4) (Walker et al., 1980) could be an underestimate. This is supported by our finding that reduction of the unstirred layer stimulates ^{14}C-fixation (Fig. 6) rather than inhibiting it. It may be that accurate modelling will have to incorporate both the charasome volume and the cell wall space.

Second, although the external electric potentials measured in the acid and alkaline regions (Walker & Smith, 1977) have been shown to be of little consequence in driving the fluxes of OH^- (Ferrier & Lucas, 1979), it should not be concluded that this is also true for the HCO_3^- situation, especially within the wall. These potentials will influence the diffusion of HCO_3^-/CO_2 and charged buffers; that this is an important effect has been shown both experimentally and theoretically by Meldon, Smith and Colton (1977). Although Ferrier (1980) suggested that the influence of this external potential and the surface potential of the membrane had little effect, this aspect warrants further investigation. While it may not be easy or possible, at present, to incorporate these changes into the computer models, it certainly makes clear the complexity of biological systems.

Why Does Chara Maintain Acid and Alkaline Regions?

We feel that our present results invalidate the proposal that *Chara* establishes discrete acid and alkaline regions along the cell wall to enable the acquisition of exogenous carbon by CO_2 diffusion. A more valid interpretation appears to be that the cell establishes localized regions of acidity to provide a high enough H^+ concentration to drive the cotransport of HCO_3^- and Cl^-. (For evidence in support of $Cl^- - 2H^+$ cotransport *see* Sanders, 1980.) Under the alkaline conditions in which this species grows it may also be necessary to establish acid regions along the cell to enable cell wall extension.

On a more general note, it should be realized that for many aquatic organisms there is considerable evidence in support of the hypothesis that these species can utilize exogenous HCO_3^-, *per se*, rather than CO_2. (For an analysis of this literature, *see* Lucas, 1983.) The point of interest in the future will be to determine if all HCO_3^- assimilators utilize a $HCO_3^- - H^+$ cotransport mechanism, or

whether, in some species, a primary active electrogenic HCO_3^- transport system actually exists (*see*, for example, Kaplan et al., 1982). Obtaining unequivocal evidence in support of the latter mechanism may be difficult.

This study was supported by National Science Foundation Grants PCM 81-17721 and PCM 80-03133. D.S. was supported by Grant GM 15858, National Institutes of General Medical Sciences, awarded to C.L. Slayman. Thanks are also due to Ms. Carol Whitman for assistance in performing some of the pH scan experiments, and to Messrs. Young and Tallon of our Physical Plant Workshop for their excellent technical assistance.

References

Arens, K. 1933. Physiologisch polarisierter massenaustausch und photosynthese bei submersen wasserpflanzen I. *Planta* **20**:621–658

Arens, K. 1936. Physiologisch polarisierter massenaustausch und photosynthese bei submersen wasserpflanzen. II. Die Ca $(HCO_3^-)_2$-assimilation. *Jahrb. Wiss. Bot.* **83**:513–560

Browse, J.A., Dromgoole, F.I., Brown, J.M.A. 1979. Photosynthesis in the acquatic macrophyte *Egeria densa*. III. Gas exchange studies. *Aust. J. Plant Physiol.* **6**:499–512

Ferrier, J.M. 1980. Apparent bicarbonate uptake and possible plasmalemma proton efflux in *Chara corallina*. *Plant Physiol.* **66**:1198–1199

Ferrier, J.M., Lucas, W.J. 1979. Plasmalemma transport of OH^- in *Chara corallina*. II. Further analysis of the diffusion system associated with OH^- efflux. *J. Exp. Bot.* **30**:705–718

Franceschi, V.R., Lucas, W.J. 1980. Structure and possible function(s) of charasomes; complex plasmalemma-cell wall elaborations present in some Characean species. *Protoplasma* **104**:253–271

Franceschi, V.R., Lucas, W.J. 1982. The relationship of the charasome to chloride uptake in *Chara corallina:* Physiological and histochemical investigations. *Planta* **154**:525–537

Gutknecht, J., Tosteson, D.C. 1973. Diffusion of weak acids across lipid bilayer membranes: Effects of chemical reactions in the unstirred layers. *Science* **182**:1258–1260

Hood, D.W., Park, K. 1962. Bicarbonate utilization by marine phytoplankton in photosynthesis. *Physiol. Plant.* **15**:273–282

Jaffe, L.F., Nuccitelli, R. 1974. An ultrasensitive vibrating probe for measuring extracellular currents. *J. Cell Biol.* **63**:614–628

Kaplan, A., Zenvirth, D., Reinhold, L., Berry, J.A. 1982. Involvement of a primary electrogenic pump in the mechanism for HCO_3^- uptake by the Cyanobacterium *Anabaena variabilis*. *Plant Physiol.* **69**:978–982

Lucas, W.J. 1975. Photosynthetic fixation of ^{14}carbon by internodal cells of *Chara corallina*. *J. Exp. Bot.* **26**:331–346

Lucas, W.J. 1976. Plasmalemma transport of HCO_3^- and OH^- in *Chara corallina:* non-antiporter systems. *J. Exp. Bot.* **27**:19–31

Lucas, W.J. 1977. Analogue inhibition of the active HCO_3^- transport site in the characean plasma membrane. *J. Exp. Bot.* **28**:1321–1336

Lucas, W.J. 1982. Mechanism of acquisition of exogenous HCO_3^- by internodal cells of *Chara corallina*. *Planta* **156**:181–192

Lucas, W.J. 1983. Photosynthetic assimilation of exogenous HCO_3^- by aquatic plants. *Annu. Rev. Plant Physiol.* **34**:71–104

Lucas, W.J., Dainty, J. 1977. HCO_3^- influx across the plasmalemma of *Chara corallina:* Divalent cation requirement. *Plant Physiol.* **60**:862–867

Lucas, W.J., Nuccitelli, R. 1980. HCO_3^- and OH^- transport across the plasmalemma of *Chara corallina:* Spatial resolution obtained using extracellular vibrating probe. *Planta* **150**:120–131

Lucas, W.J., Smith, F.A. 1973. The formation of alkaline and acid regions at the surface of *Chara corallina* cells. *J. Exp. Bot.* **24**:1–14

Marcus, Y., Zenvirth, D., Harel, E., Kaplan, A. 1982. Induction of HCO_3^- transporting capability and high photosynthetic affinity to inorganic carbon by low concentration of CO_2 in *Anabaena variabilis*. *Plant Physiol.* **69**:1008–1012

Meldon, J.H., Smith, K.A., Colton, C.K. 1977. The effect of weak acids upon the transport of carbon dioxide in alkaline solutions. *Chem. Eng. Sci.* **32**:939–950

Miller, A.G., Colman, B. 1980. Evidence for HCO_3^- transport by the blue-green alga (Cyanobacterium) *Coccochloris peniocystis*. *Plant Physiol.* **65**:397–402

Österlind, S. 1949. Growth conditions of the alga *Scenedesmus quadricauda* with special reference to the inorganic carbon sources. *Symb. Bot. Ups.* **10**:1–141

Prins, H.B.A, Snel, J.F.H., Helder, R.J., Zanstra, P.E. 1979. Photosynthetic bicarbonate utilization in the aquatic angiosperms *Potamogeton* and *Elodea*. *Hydrobiol. Bull.* **13**:106–111

Prins, H.B.A., Snel, J.F.H., Helder, R.J., Zanstra, P.E. 1980. Photosynthetic HCO_3^- utilization and OH^- excretion in aquatic angiosperms: Light-induced pH changes at the leaf surface. *Plant Physiol.* **66**:818–822

Prins, H.B.A., Snel, J.F.H., Zanstra, P.E., Helder, R.J. 1982. The mechanism of bicarbonate assimilation by the polar leaves of *Potamogeton* and *Elodea*. CO_2 concentrations at the leaf surface. *Plant Cell Environ.* **5**:207–214

Raven, J.A. 1968. The mechanism of photosynthetic use of bicarbonate by *Hydrodictyon africanum*. *J. Exp. Bot.* **19**:193–206

Raven, J.A. 1970. Exogenous inorganic carbon sources in plant photosynthesis. *Biol. Rev.* **45**:167–221

Ruttner, F. 1947. Zur frage der karbonatassimilation der wasserpflanzen. I. Teil: Die beiden haupttypen der kohlenstoffaufnahme. *Oesterr. Bot. Z.* **94**:265–294

Sanders, D. 1980. The mechanism of Cl^- transport at the plasma membrane of *Chara corallina:* I. Cotransport with H^+. *J. Membrane Biol.* **53**:129–141

Sanders, D., Slayman, C.L. 1982. Control of intracellular pH: Predominate role of oxidative metabolism, not proton transport in the eukaryotic microorganism *Neurospora*. *J. Gen. Physiol.* **80**:377–402

Smith, F.A. 1968. Rates of photosynthesis in Characean cells. II. Photosynthetic $^{14}CO_2$ fixation and ^{14}C-bicarbonate uptake by Characean cells. *J. Exp. Bot.* **19**:207–217

Smith, F.A., Walker, N.A. 1980. Photosynthesis by aquatic plants: Effects of unstirred layers in relation to assimilation of CO_2 and HCO_3^- and to carbon isotopic discrimination. *New Phytol.* **86**:245–259

Spanswick, R.M. 1981. Electrogenic ion pumps. *Annu. Rev. Plant Physiol.* **32**:267–289

Spear, D.G., Barr, J.K., Barr, C.E. 1969. Localization of hydrogen ion and chloride ion fluxes in *Nitella*. *J. Gen. Physiol.* **54**:397–414

Steemann-Nielsen, E. 1947. Photosynthesis of aquatic plants

with special reference to the carbon sources. *Dan. Bot. Ark.* **12**:1–71

Steemann-Nielsen, E. 1960. Uptake of carbon dioxide by the plant. *In:* Encyclopedia of Plant Physiology. W. Ruhland, editor. Vol. 5/1, pp. 70–84. Springer-Verlag, Berlin

Steemann-Nielsen, E. 1963. On bicarbonate utilization by marine phytoplankton in photosynthesis. With a note on carbamino carboxylic acids as a carbon source. *Physiol. Plant.* **16**:466–469

Streeter, V.L. 1958. Fluid Mechanics. McGraw-Hill, New York

Talling, J.F. 1976. The depletion of carbon dioxide from lake water by phytoplankton. *J. Ecol.* **64**:79–121

Thomas, R.C. 1978. Ion-Sensitive Intracellular Microelectrodes: How to Make and Use Them. Academic Press, London, pp. 32–44

Walker, N.A., Smith, F.A. 1977. Circulating electric currents between acid and alkaline zones associated with HCO_3^- assimilation in *Chara*. *J. Exp. Bot.* **28**:1190–1206

Walker, N.A., Smith, F.A., Cathers, I.R. 1980. Bicarbonate assimilation by fresh-water charophytes and higher plants: I. Membrane transport of bicarbonate ions is not proven. *J. Membrane Biol.* **57**:51–58

Watt, W.D., Paasche, E. 1963. An investigation of the conditions for distinguishing between CO_2 and bicarbonate utilization by algae according to the methods of Hood and Park. *Physiol. Plant.* **16**:674–681

Received 24 August 1982; revised 3 December 1982